Effects of Seal Geometry on Adhesive Stresses in Pavement Joint Seals

CHI-PING WANG AND FRANK E. WEISGERBER

Highway pavement joint seals have displayed a high incidence of adhesion failure. To predict effectively the adhesive stresses at the interface with the pavement and to promote a better understanding of the fundamentals of seal behavior, a constitutive law using the internal state variable method is developed and applied to perform stress analysis of joint seals. Special consideration is given to representing the viscoelastic nature of the sealant material. Seven seal configurations—including rectangular seals with three aspect ratios, a trapezoidal seal, and a seal with concave top and bottom surfaces—are considered. The emphasis is to describe the effects of variations in seal geometry on the adhesive stresses.

To be fully effective, poured-in-place highway pavement joint seals must adhere to the pavement. However, these seals have traditionally displayed an unacceptably high incidence of adhesion failure. Many field trials, laboratory studies, and material research programs—especially those in the past two decades—have made significant contributions to resolving this difficulty. Methods of joint preparation have been improved, materials have been enhanced to give more tenacious adhesion, and the importance of seal geometry has been recognized. But adhesion failure is still the primary cause of seal failure. Further development of seal technology is needed, which requires a more comprehensive understanding of the fundamental behavior of seal systems and sealant materials.

An obvious approach to investigating the fundamental behavior of seals would be to initiate an intensive program of experimental studies. Because difficulties such as adhesion failure begin in very localized regions, these experimental studies would need, in effect, to view the response of the seals on practically a microscopic level to ascertain the distribution and intensities of strains and stresses along with other features of seal response under a wide variety of circumstances. Such experimental studies are typically expensive. Considering the especially complex nature of the sealant material properties and the circumstances of the seals, these studies would require technically advanced experimental techniques and equipment.

Faced with analogous obstacles to performing comprehensive experimental studies of complex systems, investigators in other areas of engineering have relied on numerical stress analyses, based on the finite element method, to provide the desired microscopic view of response. It is reasonable to expect that similar stress analyses could provide valuable information on the behavior of seals. There have been few previous attempts at performing numerical analyses of seal systems because (a) none of the commercially available analysis packages includes options that adequately model the essential features of the seal system, and (b) the fundamental material properties of the sealants have not been sufficiently quantified.

This paper presents results from a comprehensive research project that was initiated specifically to develop capabilities to perform stress analysis of seal systems. The project included

- Developing a new material model along with a compatible solution strategy based on the finite element analysis method,
- Designing and conducting a testing program to evaluate the required material constants,
- Testing laboratory specimens that represent actual joints,
- Conducting a series of numerical analyses to predict the response of seals that are subjected to imposed joint deformations, and
- Comparing the results from the numerical analyses with the response of laboratory specimens.

This paper concentrates on describing the effect of seal geometry on the normal and shear stresses in the sealant at the interface with the pavement. Additional results, along with details concerning the derived constitutive equations, the testing procedure, and the finite element methodology, are available elsewhere (*1*) and will appear in other publications.

NATURE OF PROBLEM

Although the joint seal appears to be a very simple system, numerical stress analysis is complicated by the unique and challenging nature of the material involved. The materials commonly used for pavement joint seals—such as polymer-modified asphalt, silicone, and polyurethane—are all low-modulus materials that are nearly incompressible. The materials are viscoelastic and stress-relax so rapidly that significant relaxation occurs simultaneously with load application. The latter factor alone complicates testing for fundamental properties and places stringent requirements on the numerical solution strategy as well as on the form of the material model.

Even aside from the peculiarities of the materials, the seals are subjected to a special set of circumstances. The seal is in a state of plane strain so that one must consider a three-dimensional state of stress. Joint displacements, rather than applied forces, are applied to the system and the seal is subjected to very high strains under ordinary service conditions.

C.-P. Wang, Graduate Institute of Civil and Hydraulic Engineering, Fung Chia University, Taichung, Taiwan, Republic of China. F. E. Weisgerber, Department of Civil and Environmental Engineering, University of Cincinnati, Cincinnati, Ohio 45221.

PREVIOUS WORK

The earliest noteworthy attempt to investigate stresses within a seal system is the work by Tons (*2*). Using classical techniques, as opposed to numerical techniques employing discretization, Tons treated the material as elastic and incompressible and based his analysis on the premise that the seal cross section, originally a rectangle, deformed such that the top and bottom surfaces became parabolas as the seal was stretched but maintained a constant volume.

Catsiff et al. completed the most sophisticated and comprehensive of the previous studies (*3–5*). They defined the material on a fundamental level and performed detailed experimental studies to determine the constants required for their constitutive relationship. They showed that very high stresses may occur at specific points within the seals and along the interface with the substrate.

Recently, Khuri and Tons reported finite element analyses treating the sealant as an incompressible hyperelastic material to determine the distribution of strain throughout the sealant and along the interface between the sealant and pavement (*6*).

The need for the capability to perform stress analyses of low-modulus seals has also been noted by those concerned with perimeter seals for buildings and seals for glazing. Myers, for example, has analyzed fillet-type seals (*7*), and Gutowski has performed a series of theoretical and experimental studies of adhesive stresses (*8*).

MATERIAL MODEL

For stress analysis of low-modulus seal systems, the viscoelastic nature of the material is a primary factor in selecting the material model. Several theories of viscoelastic behavior have been developed over the years, but each of these traditional theories includes certain disadvantages relative to numerical analysis of seal systems. Consequently, the state variable theory was chosen because it has sufficient generality and it is computationally efficient. The state variable theory has been used previously to model creep in metal systems, but this appears to be the first application to materials characterized as amorphous cross-linked polymers.

The internal state variable method used here employs a rate-type constitutive equation for computational efficiency. This rate-type model assumes that the inelastic (creep) strain rate is a function of the current state of stress and the so-called internal state variables that represent the history-dependent nature of the materials.

A strain rate equation and one or more evolution equations are required for the state variable method. The forms of the evolution equations of the internal state variables are determined heuristically or from phenomenological theory. A generalized Maxwell model forms the basis for the incremental-type constitutive law used in the present analyses that implies a linearly viscoelastic material as generally assumed for amorphous polymers. Mechanical tests are required to determine the material constants used in the evolution equations. Details concerning the constitutive equations are omitted from this paper because of constraints on space. The equations are presented and fully discussed elsewhere (*1*).

MATERIAL CONSTANTS

The material models employed in these analyses require that moduli (E_k), relaxation times (τ_k), and Poisson's ratio (ν) be quantified. Therefore a material testing program was designed and executed. The tests were completed using Dow Corning 888 silicone joint sealant because this material has been used in previous experimental studies by others and is often used in field applications.

The specimens used for ASTM bond tests are inadequate to determine the basic material properties of a sealant material because a very complex stress field occurs within the material when the short specimen with large cross section is extended. Consequently, the tests to determine the required constants employed a specimen that was ½ × ½ in. (12 × 12 mm) in cross section and about 2.5 in. (60 mm) long. These specimens were extended at a predetermined strain rate and the induced stresses were recorded. From the continuous record of the variations of stress and strain with time, it was possible to extract the required constants by a curve-fitting process.

The tests to determine Poisson's ratio used a dumbbell-shaped specimen stamped from a thin sheet of sealant material. This specimen was extended under a microscope so that the longitudinal and transverse strains could be accurately measured and then used to calculate Poisson's ratio. An incremental approach to this calculation is required because large strains are achieved. On the basis of these tests, a value of 0.471 was used for the finite element analyses.

To verify the material model and the finite element solution strategy to the fullest extent possible, laboratory tests were also conducted using specimens in the form of rectangular seals. These were subjected to tensile and shearing-type joint deformations. The experimental results and the analytical results agreed very well, providing a basis for a high level of confidence in the analytical results.

SOLUTION STRATEGY

An incremental finite element solution strategy is used to complete the analyses. Displacements associated with a ramp-type loading history are applied incrementally in accord with the time-displacement history to be investigated. Because of the geometric nonlinearity associated with large strain behavior and the time-dependent character of the material response, a Newton-Raphson iteration method must be used within each increment in order to maintain equilibrium of internal forces. After the target displacement is achieved, that displacement is held constant while time progresses and stress relaxation continues.

CASES INVESTIGATED

Analyses were performed to determine the magnitudes and distributions of adhesive stresses in seals with the geometric configurations identified in Figure 1. To isolate the effects of geometric configuration, all other variables that would affect the stresses were held constant throughout these analyses.

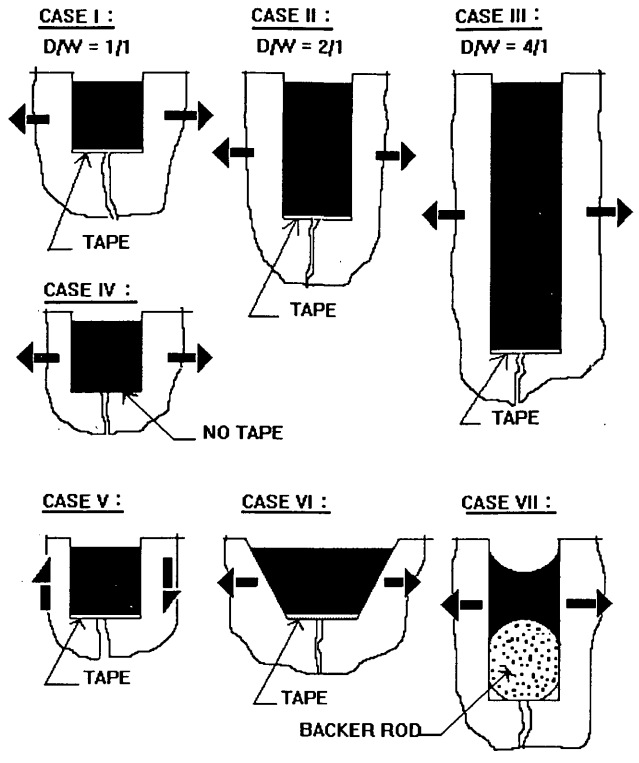

FIGURE 1 Seal cases analyzed.

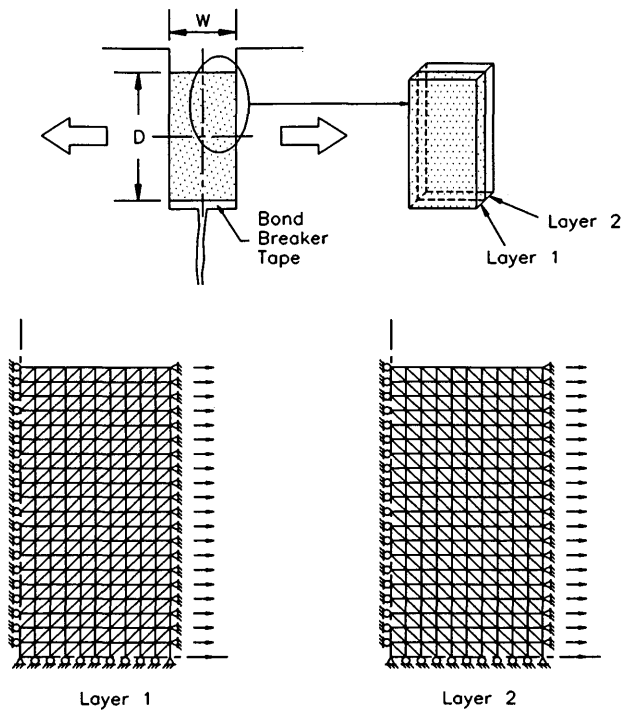

FIGURE 2 Example finite element mesh for Case II: *top*, sealant cross section; *bottom*, finite element mesh.

Therefore in all of the following cases,

- The seal width (W) is taken as 0.5 in. (12 mm),
- The joint deformation is applied at a constant rate of 0.125 in./min (3 mm/min.),
- The material constants (E_k, τ_k, and ν) were identical in all cases, and
- The level of finite element mesh refinement is held as constant as possible.

A representative mesh is shown in Figure 2, for a rectangular seal with a depth-to-width ratio, D/W, of 2/1. Two superimposed levels of triangular elements were used in all cases to eliminate the geometric bias that often occurs when using triangular elements. Because the rectangular seal is bisymmetrical, it is generally possible to work with a model that represents one-quarter of the entire seal section. As seen in Figure 2, only horizontal displacements are restrained along the vertical line of symmetry and only vertical displacements are restrained along the horizontal line of symmetry. The displacements are fully restrained along the vertical interface between sealant and substrate.

Prescribed increments of displacement are introduced uniformly along the vertical interface, as represented by the arrows in Figure 2. These displacements are temporally discretized to represent a ramp loading function from zero to maximum displacement at a constant rate. The stresses reported in the following section are those that exist when the target strain is first achieved and incorporate the effects of stress relaxation accumulated while the displacements are introduced.

RESULTS

Rectangular Seals

Five analyses were performed for rectangular seals (Cases I through V in Figure 1). To investigate the significance of the aspect ratio (D/W) on adhesion stress magnitudes and distributions, seals with D/W = 1/1, 2/1, and 4/1 were analyzed. For these three, the bottom surface of the seal is assumed to be free of adhesion due to the use of a bond-breaking tape. The fourth rectangular seal has D/W = 1/1 and is bonded to the bottom of the reservoir (no bond-breaking tape). Case V is also a seal with D/W = 1/1 and with bond-breaking tape but was analyzed for shear-type deformations rather than the tensile deformations imposed in all other cases.

Case I

The normal and shear adhesive stress distributions at the vertical seal-substrate interface for the square seal subjected to tensile-type joint deformations are shown in Figure 3; D/W = 1/1. The results for joint strains of 1, 6, and 12.5 percent clearly show that the stress magnitudes are not proportional to applied deformation. This is primarily due to the viscoelastic nature of the material: the stress relaxation that occurs while the deformation is applied is a particularly significant feature of the response. The most interesting and important observation to be made relative to the stress distributions in this first case is that there are very high stress peaks at the top and bottom of the interfacial surface.

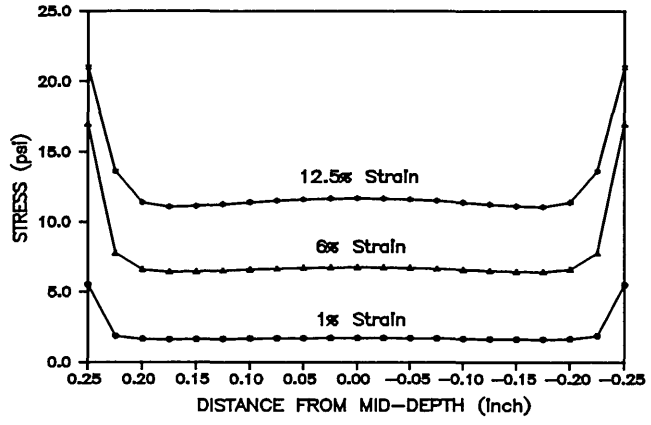

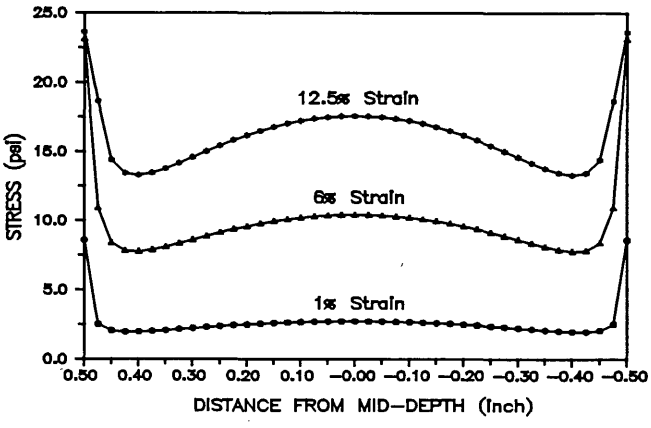

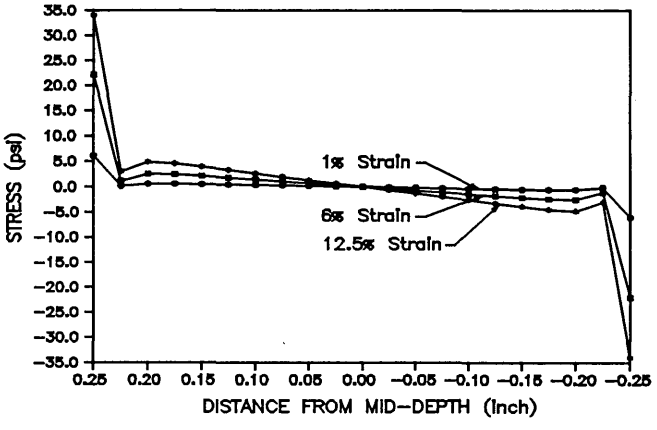

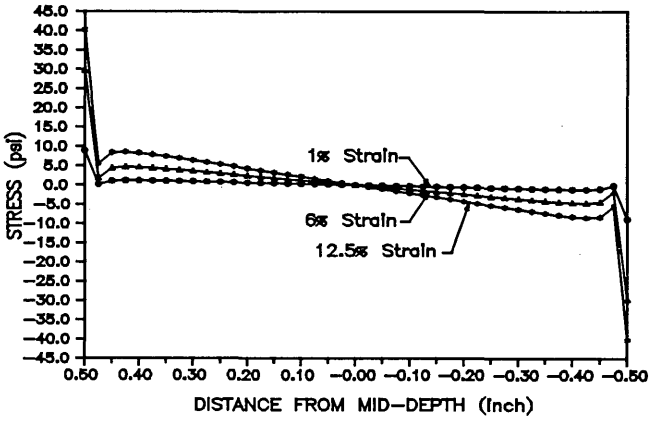

FIGURE 3 Adhesive stress distributions for Case I: *top*, normal stress; *bottom*, shear stress.

FIGURE 4 Adhesive stress distributions for Case II: *top*, normal stress; *bottom*, shear stress.

Case II

For a rectangular joint seal with $D/W = 2/1$, the normal and shear adhesion stress distributions are similar to those for Case I, but the stress magnitudes for any given joint strain are higher. The average normal stress implied by Figure 4 appears to be about 25 to 50 percent higher than that for Case I. Also, the normal stress is not as uniformly distributed over the central region of the interface, especially at higher joint strain.

Case III

Figure 5 gives the stress distributions for the rectangular seal with $D/W = 4/1$. All along the interface, the stresses are substantially greater than those for Cases I and II. Although large stress peaks are seen at the top and bottom of the interface, the maximum normal stress may be at mid-depth of the seal. Interestingly, there have been reports that failures of some ASTM bond test specimens initiate at the center of the 2- × 2-in. (50- × 50-mm) bonded surface. The sealant is 0.5 in. (12 mm) thick in these specimens, giving $D/W = 4/1$. Therefore, the results shown here may somewhat approximate the adhesion stress distributions in the ASTM bond test specimens even though the bond test specimens are not in a true state of plane strain as assumed in the present analyses.

Case IV

The fourth case, as in Case I, considers a seal with $D/W = 1/1$ subjected to tensile joint strains. Here, however, the sealant is assumed to be bonded to the bottom of the reservoir. The distributions of adhesive stresses over the vertical interface (reservoir wall) are shown in Figure 6, and the distributions of adhesive stresses along the horizontal interface at the bottom of the reservoir are shown in Figure 7. This seal has normal stresses and shear stresses along the vertical interface that are slightly higher in magnitude than those for Case I, except near the bottom of the reservoir wall where the stresses tend to be very small. The normal adhesion stresses along the horizontal interface [Figure 7 (*top*)] are relatively low and are necessarily zero at the center of the seal where the sealant is spans the presumed crack. On the other hand, the shear adhesive stress at the horizontal interface [Figure 7 (*bottom*)] has a very high magnitude near the crack.

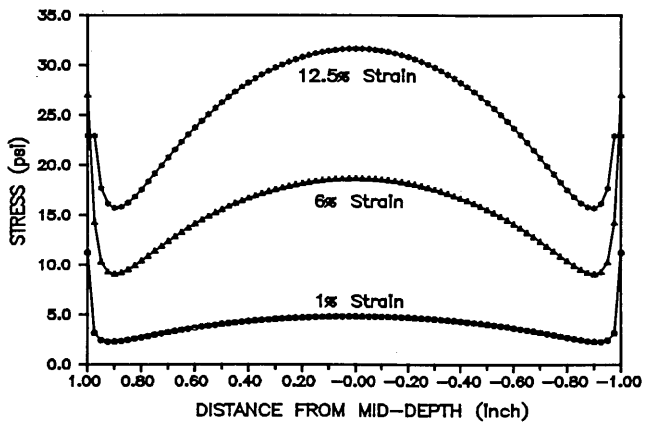

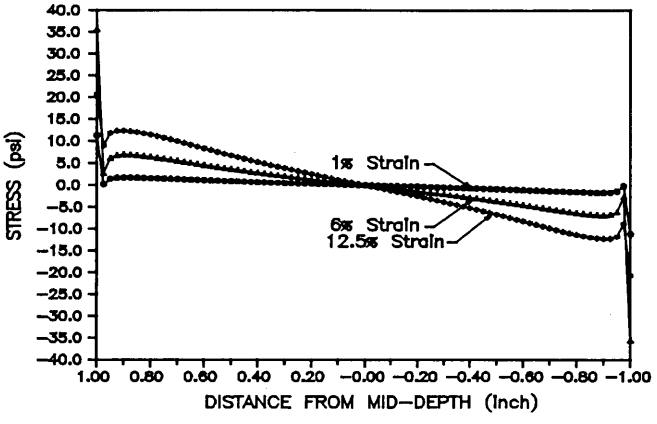

FIGURE 5 Adhesive stress distributions for Case III: *top*, normal stress; *bottom*, shear stress.

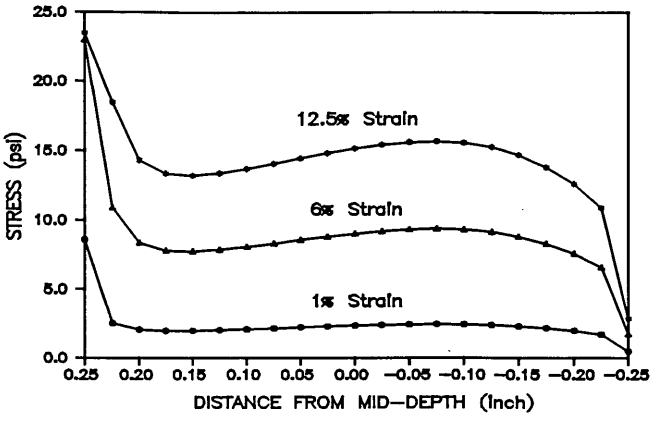

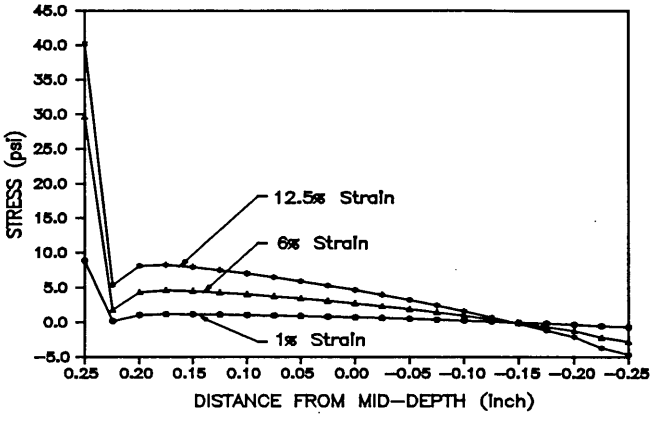

FIGURE 6 Adhesive stress distribution at wall for Case IV: *top*, normal stress; *bottom*, shear stress.

Case V

Normal and shear stress distributions due to shearing-type deformations in a seal with D/W = 1/1 are shown in Figure 8. In this case, the indicated joint strains are stated in terms of the customary definition of engineering shear strain. That is, the joint shear strain is calculated as $\gamma = \Delta_V/W$, in which Δ_V is the relative vertical displacement of the pavement to either side of the joint. The stress distributions are not symmetrical with respect to the mid-depth of the seal due to the relatively large deformations involved. (A unisymmetrical finite element model was used for this case.) As in the previous cases, stress peaks occur at the extreme top and bottom of the interface region.

Trapezoidal Seal, Case VI

The adhesive stress distributions for a seal with a trapezoidal section are shown in Figure 9: D/W = 1/1 with W as the minimum width that occurs at the bottom. The width at top of the seal is twice the width at the bottom. Peak normal and shear stresses occur only at the top of this seal, but the average stresses and peak stress magnitudes are only a little reduced from those seen in the square seal, which is Case I.

Seal with Concave Surfaces, Case VII

Figure 10 presents the normal and shear adhesive stress distributions for a seal with concave, unbonded, top, and bottom surfaces. The ratio of minimum depth to width is 1/1. The concavity is circular, based on a circle with a diameter equal to the seal width. However, for modeling purposes, the areas near the points of tangency are represented by small triangular regions. The stress distributions for Case VII are dramatically different from all the other cases: there are no high stress peaks.

DISCUSSION OF RESULTS

The stress peaks observed in all of the cases, except for the seal with concave surfaces, play a very strong role in the behavior of the seals. Obviously, an adhesive failure in a rectangular seal should be expected to initiate at the extreme top or bottom of the interface when the peak stresses attain a specific magnitude. The magnitude at which release initiates is expected to be material-specific.

Ideally, the analyses would accurately predict the magnitude at the apex of each stress peak. However, it is difficult to make a numerically accurate prediction because the finite

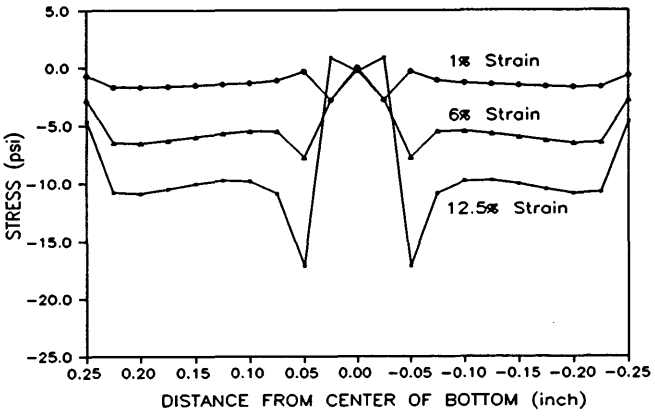

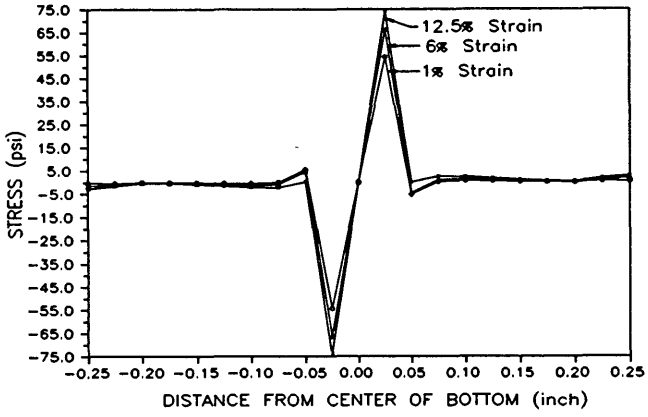

FIGURE 7 Adhesive stress distribution at bottom for Case IV: *top*, normal stress; *bottom*, shear stress.

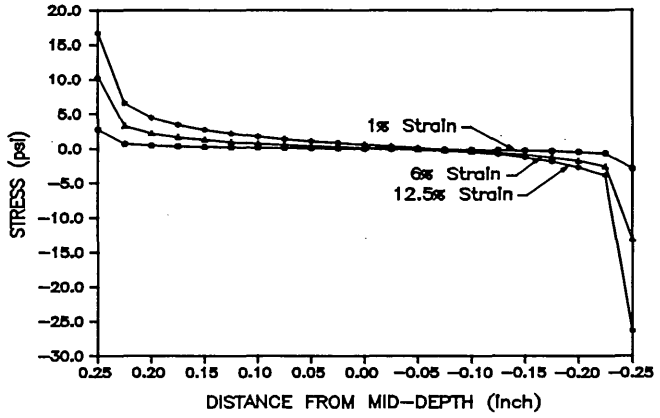

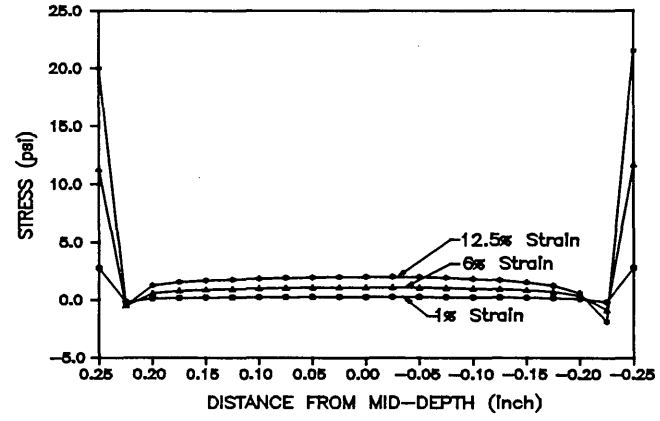

FIGURE 8 Adhesive stress distributions for Case V: *top*, normal stress; *bottom*, shear stress.

element representation of the very top and bottom points is a sharp reentrant corner that is mathematically a point of singularity in the stress function. The results of finite element analyses near points of singularity are very sensitive to the size and arrangement of the element mesh. Using smaller elements in regions with high stress gradients generally improves the solution accuracy and reliability, but refining the mesh near singular points amplifies rather than resolves the difficulty. As the element size near the singular point is reduced, the stress magnitude tends toward infinity.

Of course, the stresses cannot approach infinite magnitudes in real seal systems. Instead, as the stresses begin to get large near a singular point, the system changes geometry: it either deforms to geometry that mitigates the problem or it fractures. Low-modulus materials attempt to deform to a geometry that is similar to the seal with concave surfaces. That is, the seal surface that is initially normal to the substrate moves toward becoming tangent to the substrate, at least in a very localized region. It thus tends to take a form similar to that of the meniscus that forms in water near the sides of a container. In view of this, artificially creating menisci in rectangular seals while they are being placed may significantly enhance their performance.

Another singular point is seen in Case IV on the horizontal interface at the edge of the crack. Here again, the stress is theoretically infinite. Practically, if the adhesive stress is very high and causes debonding along the horizontal interface, the seal may approach the circumstances of Case I without having used a bond-breaking tape or backing material. Alternatively, since the internal stresses are also quite high at this point, a cohesive failure may be initiated within the material, resulting in a vertical crack reaching to the top surface of the seal. It is consequently recommended that adhesion to the bottom of the reservoir be prevented by using a bond-breaking tape or backing materials, as is the general practice.

Finally, it may be noted that the "dips" in many of the stress distribution plots near the stress peaks may be artifices that result from deducing the stress magnitudes from nodal forces along the boundaries of the finite element mesh. Extrapolation of adhesive stresses from stresses within the finite elements leads to distribution plots that do not display such dips but are otherwise similar to the distributions shown.

CONCLUSION

The results provided in preceding sections illustrate the effects of variations in seal geometry on the magnitude and distribution of adhesive stresses. It is shown that rectangular seals with low aspect ratios are preferable to those with high aspect

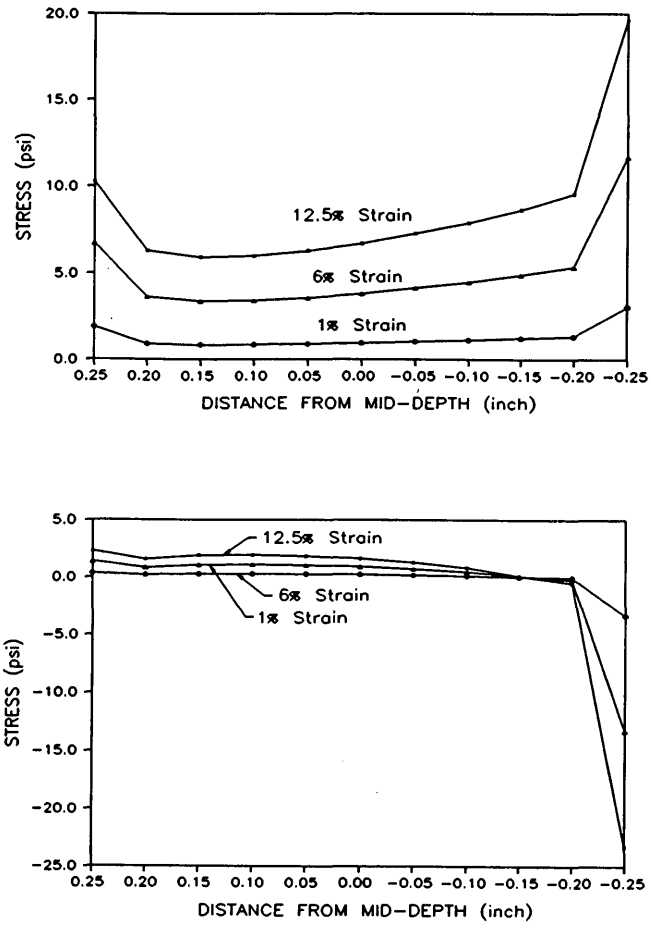

FIGURE 9 Adhesive stress distributions for Case VI: *top*, normal stress; *bottom*, shear stress.

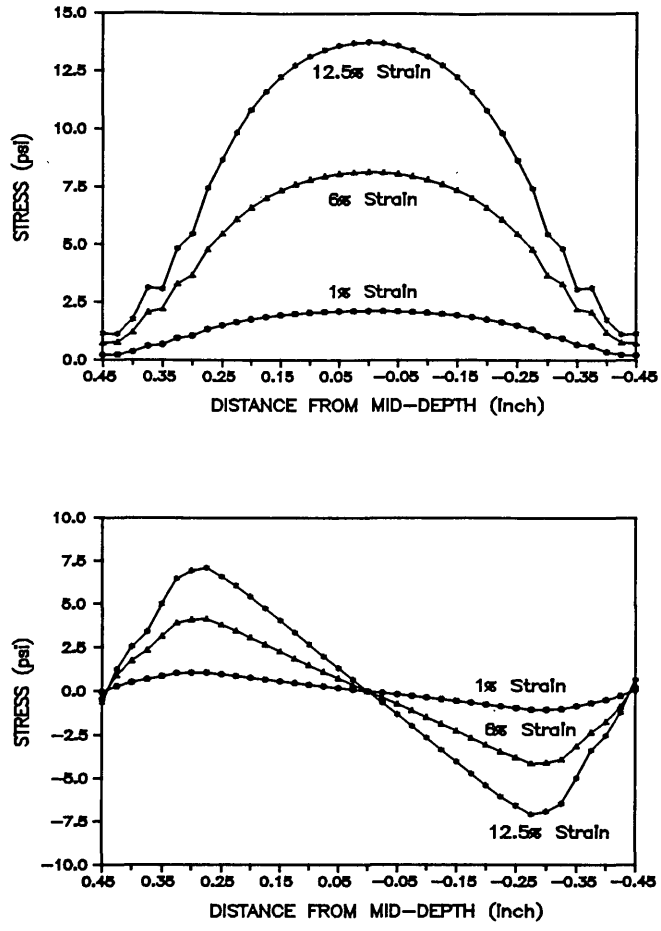

FIGURE 10 Adhesive stress distributions for Case VII, $D/W = 1/1$ and $D'/W = 2/1$: *top*, normal stress; *bottom*, shear stress.

ratios, that bonding to the bottom of the reservoir has little effect on the adhesion to the vertical walls but may lead to cohesive failure, that trapezoidal seals are apparently neither advantageous nor disadvantageous in comparison with rectangular seals, and that seals with concave upper and lower surfaces are superior to rectangular seals.

REFERENCES

1. C. P. Wang. *Development of Stress Analysis Procedure for Low-Modulus Elastomeric Sealants*. Ph.D. dissertation. University of Cincinnati, Ohio, 1992.
2. E. Tons. A Theoretical Approach to the Design of a Road Joint Seal. *Bulletin 229*, HRB, National Research Council, Washington, D.C., 1959, pp. 20–53.
3. E. H. Catsiff, R. F. Hoffman, and R. T. Kowalewski. Predicting Joint Sealant Performance by Computer Simulation. I. Justification of Method. *Journal of Applied Polymer Science*, Vol. 14, 1970, pp. 1143–1158.
4. E. H. Catsiff, R. F. Hoffman, and R. T. Kowalewski. Predicting Joint Sealant Performance by Computer Simulation. II. Results in Simple Extension and Compression. *Journal of Applied Polymer Science*, Vol. 14, 1970, pp. 1159–1178.
5. E. H. Catsiff. Predicting Joint Sealant Performance by Computer Simulation. III. Simulation of Single-and Multi-Step Extension of a Stress-Relaxing Material. *Journal of Applied Polymer Science*, Vol. 15, 1971, pp. 1021–1028.
6. M. F. Khuri and E. Tons. Comparing Rectangular and Trapezoidal Seals Using the Finite Element Method. In *Transportation Research Record 1334*, TRB, National Research Council, Washington, D.C., 1992, pp. 25–37.
7. J. C. Myers. Behavior of Fillet Sealant Joints. In *ASTM STP-1069: Building Sealants: Materials, Properties and Performance* (T. F. O'Connor, ed.), ASTM, Philadelphia, Pa., 1990, pp. 108–121.
8. W. S. Gutowski. Adhesive Properties of Silicone Sealants. In *ASTM STP-1069: Building Sealants: Materials, Properties and Performance* (T. F. O'Connor, ed.), ASTM, Philadelphia, Pa., 1990, pp. 174–192.

Publication of this paper sponsored by Committee on Sealants and Fillers for Joints and Cracks.